Search for Associated Higgs Boson Production $WH \rightarrow WWW^* \rightarrow l^{\pm}\nu l'^{\pm}\nu' + X$ in $p\bar{p}$ Collisions at $\sqrt{s} = 1.96$ TeV

V. M. Abazov,[1] B. Abbott,[76] M. Abolins,[66] B. S. Acharya,[29] M. Adams,[52] T. Adams,[50] M. Agelou,[18] J.-L. Agram,[19] S. H. Ahn,[31] M. Ahsan,[60] G. D. Alexeev,[36] G. Alkhazov,[40] A. Alton,[65] G. Alverson,[64] G. A. Alves,[2] M. Anastasoaie,[35] T. Andeen,[54] S. Anderson,[46] B. Andrieu,[17] M. S. Anzelc,[54] Y. Arnoud,[14] M. Arov,[53] A. Askew,[50] B. Åsman,[41] A. C. S. Assis Jesus,[3] O. Atramentov,[58] C. Autermann,[21] C. Avila,[8] C. Ay,[24] F. Badaud,[13] A. Baden,[62] L. Bagby,[53] B. Baldin,[51] D. V. Bandurin,[60] P. Banerjee,[29] S. Banerjee,[29] E. Barberis,[64] P. Bargassa,[81] P. Baringer,[59] C. Barnes,[44] J. Barreto,[2] J. F. Bartlett,[51] U. Bassler,[17] D. Bauer,[44] A. Bean,[59] M. Begalli,[3] M. Begel,[72] C. Belanger-Champagne,[5] L. Bellantoni,[51] A. Bellavance,[68] J. A. Benitez,[66] S. B. Beri,[27] G. Bernardi,[17] R. Bernhard,[42] L. Berntzon,[15] I. Bertram,[43] M. Besançon,[18] R. Beuselinck,[44] V. A. Bezzubov,[39] P. C. Bhat,[51] V. Bhatnagar,[27] M. Binder,[25] C. Biscarat,[43] K. M. Black,[63] I. Blackler,[44] G. Blazey,[53] F. Blekman,[44] S. Blessing,[50] D. Bloch,[19] K. Bloom,[68] U. Blumenschein,[23] A. Boehnlein,[51] O. Boeriu,[56] T. A. Bolton,[60] G. Borissov,[43] K. Bos,[34] T. Bose,[78] A. Brandt,[79] R. Brock,[66] G. Brooijmans,[71] A. Bross,[51] D. Brown,[79] N. J. Buchanan,[50] D. Buchholz,[54] M. Buehler,[82] V. Buescher,[23] S. Burdin,[51] S. Burke,[46] T. H. Burnett,[83] E. Busato,[17] C. P. Buszello,[44] J. M. Butler,[63] P. Calfayan,[25] S. Calvet,[15] J. Cammin,[72] S. Caron,[34] W. Carvalho,[3] B. C. K. Casey,[78] N. M. Cason,[56] H. Castilla-Valdez,[33] S. Chakrabarti,[29] D. Chakraborty,[53] K. M. Chan,[72] A. Chandra,[49] D. Chapin,[78] F. Charles,[19] E. Cheu,[46] F. Chevallier,[14] D. K. Cho,[63] S. Choi,[32] B. Choudhary,[28] L. Christofek,[59] D. Claes,[68] B. Clément,[19] C. Clément,[41] Y. Coadou,[5] M. Cooke,[81] W. E. Cooper,[51] D. Coppage,[59] M. Corcoran,[81] M.-C. Cousinou,[15] B. Cox,[45] S. Crépé-Renaudin,[14] D. Cutts,[78] M. Ćwiok,[30] H. da Motta,[2] A. Das,[63] M. Das,[61] B. Davies,[43] G. Davies,[44] G. A. Davis,[54] K. De,[79] P. de Jong,[34] S. J. de Jong,[35] E. De La Cruz-Burelo,[65] C. De Oliveira Martins,[3] J. D. Degenhardt,[65] F. Déliot,[18] M. Demarteau,[51] R. Demina,[72] P. Demine,[18] D. Denisov,[51] S. P. Denisov,[39] S. Desai,[73] H. T. Diehl,[51] M. Diesburg,[51] M. Doidge,[43] A. Dominguez,[68] H. Dong,[73] L. V. Dudko,[38] L. Duflot,[16] S. R. Dugad,[29] A. Duperrin,[15] J. Dyer,[66] A. Dyshkant,[53] M. Eads,[68] D. Edmunds,[66] T. Edwards,[45] J. Ellison,[49] J. Elmsheuser,[25] V. D. Elvira,[51] S. Eno,[62] P. Ermolov,[38] J. Estrada,[51] H. Evans,[55] A. Evdokimov,[37] V. N. Evdokimov,[39] S. N. Fatakia,[63] L. Feligioni,[63] A. V. Ferapontov,[60] T. Ferbel,[72] F. Fiedler,[25] F. Filthaut,[35] W. Fisher,[51] H. E. Fisk,[51] I. Fleck,[23] M. Ford,[45] M. Fortner,[53] H. Fox,[23] S. Fu,[51] S. Fuess,[51] T. Gadfort,[83] C. F. Galea,[35] E. Gallas,[51] E. Galyaev,[56] C. Garcia,[72] A. Garcia-Bellido,[83] J. Gardner,[59] V. Gavrilov,[37] A. Gay,[19] P. Gay,[13] D. Gelé,[19] R. Gelhaus,[49] C. E. Gerber,[52] Y. Gershtein,[50] D. Gillberg,[5] G. Ginther,[72] N. Gollub,[41] B. Gómez,[8] A. Goussiou,[56] P. D. Grannis,[73] H. Greenlee,[51] Z. D. Greenwood,[61] E. M. Gregores,[4] G. Grenier,[20] Ph. Gris,[13] J.-F. Grivaz,[16] S. Grünendahl,[51] M. W. Grünewald,[30] F. Guo,[73] J. Guo,[73] G. Gutierrez,[51] P. Gutierrez,[76] A. Haas,[71] N. J. Hadley,[62] P. Haefner,[25] S. Hagopian,[50] J. Haley,[69] I. Hall,[76] R. E. Hall,[48] L. Han,[7] K. Hanagaki,[51] K. Harder,[60] A. Harel,[72] R. Harrington,[64] J. M. Hauptman,[58] R. Hauser,[66] J. Hays,[54] T. Hebbeker,[21] D. Hedin,[53] J. G. Hegeman,[34] J. M. Heinmiller,[52] A. P. Heinson,[49] U. Heintz,[63] C. Hensel,[59] G. Hesketh,[64] M. D. Hildreth,[56] R. Hirosky,[82] J. D. Hobbs,[73] B. Hoeneisen,[12] H. Hoeth,[26] M. Hohlfeld,[16] S. J. Hong,[31] R. Hooper,[78] P. Houben,[34] Y. Hu,[73] Z. Hubacek,[10] V. Hynek,[9] I. Iashvili,[70] R. Illingworth,[51] A. S. Ito,[51] S. Jabeen,[63] M. Jaffré,[16] S. Jain,[76] K. Jakobs,[23] C. Jarvis,[62] A. Jenkins,[44] R. Jesik,[44] K. Johns,[46] C. Johnson,[71] M. Johnson,[51] A. Jonckheere,[51] P. Jonsson,[44] A. Juste,[51] D. Käfer,[21] S. Kahn,[74] E. Kajfasz,[15] A. M. Kalinin,[36] J. M. Kalk,[61] J. R. Kalk,[66] S. Kappler,[21] D. Karmanov,[38] J. Kasper,[63] P. Kasper,[51] I. Katsanos,[71] D. Kau,[50] R. Kaur,[27] R. Kehoe,[80] S. Kermiche,[15] S. Kesisoglou,[78] N. Khalatyan,[63] A. Khanov,[77] A. Kharchilava,[70] Y. M. Kharzheev,[36] D. Khatidze,[71] H. Kim,[79] T. J. Kim,[31] M. H. Kirby,[35] B. Klima,[51] J. M. Kohli,[27] J.-P. Konrath,[23] M. Kopal,[76] V. M. Korablev,[39] J. Kotcher,[74] B. Kothari,[71] A. Koubarovsky,[38] A. V. Kozelov,[39] J. Kozminski,[66,‡] D. Krop,[55] A. Kryemadhi,[82] T. Kuhl,[24] A. Kumar,[70] S. Kunori,[62] A. Kupco,[11] T. Kurča,[20,*] J. Kvita,[9] S. Lager,[41] S. Lammers,[71] G. Landsberg,[78] J. Lazoflores,[50] A.-C. Le Bihan,[19] P. Lebrun,[20] W. M. Lee,[53] A. Leflat,[38] F. Lehner,[42] V. Lesne,[13] J. Leveque,[46] P. Lewis,[44] J. Li,[79] Q. Z. Li,[51] J. G. R. Lima,[53] D. Lincoln,[51] J. Linnemann,[66] V. V. Lipaev,[39] R. Lipton,[51] Z. Liu,[5] L. Lobo,[44] A. Lobodenko,[40] M. Lokajicek,[11] A. Lounis,[19] P. Love,[43] H. J. Lubatti,[83] M. Lynker,[56] A. L. Lyon,[51] A. K. A. Maciel,[2] R. J. Madaras,[47] P. Mättig,[26] C. Magass,[21] A. Magerkurth,[65] A.-M. Magnan,[14] N. Makovec,[16] P. K. Mal,[56] H. B. Malbouisson,[3] S. Malik,[68] V. L. Malyshev,[36] H. S. Mao,[6] Y. Maravin,[60] M. Martens,[51] S. E. K. Mattingly,[78] R. McCarthy,[73] D. Meder,[24] A. Melnitchouk,[67] A. Mendes,[15] L. Mendoza,[8] M. Merkin,[38] K. W. Merritt,[51] A. Meyer,[21] J. Meyer,[22] M. Michaut,[18] H. Miettinen,[81] T. Millet,[20] J. Mitrevski,[71] J. Molina,[3] N. K. Mondal,[29] J. Monk,[45] R. W. Moore,[5] T. Moulik,[59] G. S. Muanza,[16] M. Mulders,[51] M. Mulhearn,[71] L. Mundim,[3] Y. D. Mutaf,[73] E. Nagy,[15] M. Naimuddin,[28] M. Narain,[63] N. A. Naumann,[35] H. A. Neal,[65] J. P. Negret,[8] S. Nelson,[50] P. Neustroev,[40] C. Noeding,[23] A. Nomerotski,[51] S. F. Novaes,[4] T. Nunnemann,[25] V. O'Dell,[51] D. C. O'Neil,[5] G. Obrant,[40]

151804-1

V. Oguri,[3] N. Oliveira,[3] N. Oshima,[51] R. Otec,[10] G. J. Otero y Garzón,[52] M. Owen,[45] P. Padley,[81] N. Parashar,[57] S.-J. Park,[72] S. K. Park,[31] J. Parsons,[71] R. Partridge,[78] N. Parua,[73] A. Patwa,[74] G. Pawloski,[81] P. M. Perea,[49] E. Perez,[18] K. Peters,[45] P. Pétroff,[16] M. Petteni,[44] R. Piegaia,[1] M.-A. Pleier,[22] P. L. M. Podesta-Lerma,[33] V. M. Podstavkov,[51] Y. Pogorelov,[56] M.-E. Pol,[2] A. Pompoš,[76] B. G. Pope,[66] A. V. Popov,[39] W. L. Prado da Silva,[3] H. B. Prosper,[50] S. Protopopescu,[74] J. Qian,[65] A. Quadt,[22] B. Quinn,[67] K. J. Rani,[29] K. Ranjan,[28] P. N. Ratoff,[43] P. Renkel,[80] S. Reucroft,[64] M. Rijssenbeek,[73] I. Ripp-Baudot,[19] F. Rizatdinova,[77] S. Robinson,[44] R. F. Rodrigues,[3] C. Royon,[18] P. Rubinov,[51] R. Ruchti,[56] V. I. Rud,[38] G. Sajot,[14] A. Sánchez-Hernández,[33] M. P. Sanders,[62] A. Santoro,[3] G. Savage,[51] L. Sawyer,[61] T. Scanlon,[44] D. Schaile,[25] R. D. Schamberger,[73] Y. Scheglov,[40] H. Schellman,[54] P. Schieferdecker,[25] C. Schmitt,[26] C. Schwanenberger,[45] A. Schwartzman,[69] R. Schwienhorst,[66] S. Sengupta,[50] H. Severini,[76] E. Shabalina,[52] M. Shamim,[60] V. Shary,[18] A. A. Shchukin,[39] W. D. Shephard,[56] R. K. Shivpuri,[28] D. Shpakov,[51] V. Siccardi,[19] R. A. Sidwell,[60] V. Simak,[10] V. Sirotenko,[51] P. Skubic,[76] P. Slattery,[72] R. P. Smith,[51] G. R. Snow,[68] J. Snow,[75] S. Snyder,[74] S. Söldner-Rembold,[45] X. Song,[53] L. Sonnenschein,[17] A. Sopczak,[43] M. Sosebee,[79] K. Soustruznik,[9] M. Souza,[2] B. Spurlock,[79] J. Stark,[14] J. Steele,[61] V. Stolin,[37] A. Stone,[52] D. A. Stoyanova,[39] J. Strandberg,[41] M. A. Strang,[70] M. Strauss,[76] R. Ströhmer,[25] D. Strom,[54] M. Strovink,[47] L. Stutte,[51] S. Sumowidagdo,[50] A. Sznajder,[3] M. Talby,[15] P. Tamburello,[46] W. Taylor,[5] P. Telford,[45] J. Temple,[46] B. Tiller,[25] M. Titov,[23] V. V. Tokmenin,[36] M. Tomoto,[51] T. Toole,[62] I. Torchiani,[23] S. Towers,[43] T. Trefzger,[24] S. Trincaz-Duvoid,[17] D. Tsybychev,[73] B. Tuchming,[18] C. Tully,[69] A. S. Turcot,[45] P. M. Tuts,[71] R. Unalan,[66] L. Uvarov,[40] S. Uvarov,[40] S. Uzunyan,[53] B. Vachon,[5] P. J. van den Berg,[34] R. Van Kooten,[55] W. M. van Leeuwen,[34] N. Varelas,[52] E. W. Varnes,[46] A. Vartapetian,[79] I. A. Vasilyev,[39] M. Vaupel,[26] P. Verdier,[20] L. S. Vertogradov,[36] M. Verzocchi,[51] F. Villeneuve-Seguier,[44] P. Vint,[44] J.-R. Vlimant,[17] E. Von Toerne,[60] M. Voutilainen,[68,†] M. Vreeswijk,[34] H. D. Wahl,[50] L. Wang,[62] J. Warchol,[56] G. Watts,[83] M. Wayne,[56] M. Weber,[51] H. Weerts,[66] N. Wermes,[22] M. Wetstein,[62] A. White,[79] D. Wicke,[26] G. W. Wilson,[59] S. J. Wimpenny,[49] M. Wobisch,[51] J. Womersley,[51] D. R. Wood,[64] T. R. Wyatt,[45] Y. Xie,[78] N. Xuan,[56] S. Yacoob,[54] R. Yamada,[51] M. Yan,[62] T. Yasuda,[51] Y. A. Yatsunenko,[36] K. Yip,[74] H. D. Yoo,[78] S. W. Youn,[54] C. Yu,[14] J. Yu,[79] A. Yurkewicz,[73] A. Zatserklyaniy,[53] C. Zeitnitz,[26] D. Zhang,[51] T. Zhao,[83] B. Zhou,[65] J. Zhu,[73] M. Zielinski,[72] D. Zieminska,[55] A. Zieminski,[55] V. Zutshi,[53] and E. G. Zverev[38]

(D0 Collaboration)

[1]*Universidad de Buenos Aires, Buenos Aires, Argentina*
[2]*LAFEX, Centro Brasileiro de Pesquisas Físicas, Rio de Janeiro, Brazil*
[3]*Universidade do Estado do Rio de Janeiro, Rio de Janeiro, Brazil*
[4]*Instituto de Física Teórica, Universidade Estadual Paulista, São Paulo, Brazil*
[5]*University of Alberta, Edmonton, Alberta, Canada,*
Simon Fraser University, Burnaby, British Columbia, Canada,
York University, Toronto, Ontario, Canada, and McGill University, Montreal, Quebec, Canada
[6]*Institute of High Energy Physics, Beijing, People's Republic of China*
[7]*University of Science and Technology of China, Hefei, People's Republic of China*
[8]*Universidad de los Andes, Bogotá, Colombia*
[9]*Center for Particle Physics, Charles University, Prague, Czech Republic*
[10]*Czech Technical University, Prague, Czech Republic*
[11]*Center for Particle Physics, Institute of Physics, Academy of Sciences of the Czech Republic, Prague, Czech Republic*
[12]*Universidad San Francisco de Quito, Quito, Ecuador*
[13]*Laboratoire de Physique Corpusculaire, IN2P3-CNRS, Université Blaise Pascal, Clermont-Ferrand, France*
[14]*Laboratoire de Physique Subatomique et de Cosmologie, IN2P3-CNRS, Universite de Grenoble 1, Grenoble, France*
[15]*CPPM, IN2P3-CNRS, Université de la Méditerranée, Marseille, France*
[16]*IN2P3-CNRS, Laboratoire de l'Accélérateur Linéaire, Orsay, France*
[17]*LPNHE, IN2P3-CNRS, Universités Paris VI and VII, Paris, France*
[18]*DAPNIA/Service de Physique des Particules, CEA, Saclay, France*
[19]*IPHC, IN2P3-CNRS, Université Louis Pasteur, Strasbourg, France,*
and Université de Haute Alsace, Mulhouse, France
[20]*Institut de Physique Nucléaire de Lyon, IN2P3-CNRS, Université Claude Bernard, Villeurbanne, France*
[21]*III. Physikalisches Institut A, RWTH Aachen, Aachen, Germany*
[22]*Physikalisches Institut, Universität Bonn, Bonn, Germany*
[23]*Physikalisches Institut, Universität Freiburg, Freiburg, Germany*
[24]*Institut für Physik, Universität Mainz, Mainz, Germany*
[25]*Ludwig-Maximilians-Universität München, München, Germany*
[26]*Fachbereich Physik, University of Wuppertal, Wuppertal, Germany*

[27]Panjab University, Chandigarh, India
[28]Delhi University, Delhi, India
[29]Tata Institute of Fundamental Research, Mumbai, India
[30]University College Dublin, Dublin, Ireland
[31]Korea Detector Laboratory, Korea University, Seoul, Korea
[32]SungKyunKwan University, Suwon, Korea
[33]CINVESTAV, Mexico City, Mexico
[34]FOM-Institute NIKHEF and University of Amsterdam/NIKHEF, Amsterdam, The Netherlands
[35]Radboud University Nijmegen/NIKHEF, Nijmegen, The Netherlands
[36]Joint Institute for Nuclear Research, Dubna, Russia
[37]Institute for Theoretical and Experimental Physics, Moscow, Russia
[38]Moscow State University, Moscow, Russia
[39]Institute for High Energy Physics, Protvino, Russia
[40]Petersburg Nuclear Physics Institute, St. Petersburg, Russia
[41]Lund University, Lund, Sweden,
Royal Institute of Technology and Stockholm University, Stockholm, Sweden,
and Uppsala University, Uppsala, Sweden
[42]Physik Institut der Universität Zürich, Zürich, Switzerland
[43]Lancaster University, Lancaster, United Kingdom
[44]Imperial College, London, United Kingdom
[45]University of Manchester, Manchester, United Kingdom
[46]University of Arizona, Tucson, Arizona 85721, USA
[47]Lawrence Berkeley National Laboratory and University of California, Berkeley, California 94720, USA
[48]California State University, Fresno, California 93740, USA
[49]University of California, Riverside, California 92521, USA
[50]Florida State University, Tallahassee, Florida 32306, USA
[51]Fermi National Accelerator Laboratory, Batavia, Illinois 60510, USA
[52]University of Illinois at Chicago, Chicago, Illinois 60607, USA
[53]Northern Illinois University, DeKalb, Illinois 60115, USA
[54]Northwestern University, Evanston, Illinois 60208, USA
[55]Indiana University, Bloomington, Indiana 47405, USA
[56]University of Notre Dame, Notre Dame, Indiana 46556, USA
[57]Purdue University Calumet, Hammond, Indiana 46323, USA
[58]Iowa State University, Ames, Iowa 50011, USA
[59]University of Kansas, Lawrence, Kansas 66045, USA
[60]Kansas State University, Manhattan, Kansas 66506, USA
[61]Louisiana Tech University, Ruston, Louisiana 71272, USA
[62]University of Maryland, College Park, Maryland 20742, USA
[63]Boston University, Boston, Massachusetts 02215, USA
[64]Northeastern University, Boston, Massachusetts 02115, USA
[65]University of Michigan, Ann Arbor, Michigan 48109, USA
[66]Michigan State University, East Lansing, Michigan 48824, USA
[67]University of Mississippi, University, Mississippi 38677, USA
[68]University of Nebraska, Lincoln, Nebraska 68588, USA
[69]Princeton University, Princeton, New Jersey 08544, USA
[70]State University of New York, Buffalo, New York 14260, USA
[71]Columbia University, New York, New York 10027, USA
[72]University of Rochester, Rochester, New York 14627, USA
[73]State University of New York, Stony Brook, New York 11794, USA
[74]Brookhaven National Laboratory, Upton, New York 11973, USA
[75]Langston University, Langston, Oklahoma 73050, USA
[76]University of Oklahoma, Norman, Oklahoma 73019, USA
[77]Oklahoma State University, Stillwater, Oklahoma 74078, USA
[78]Brown University, Providence, Rhode Island 02912, USA
[79]University of Texas, Arlington, Texas 76019, USA
[80]Southern Methodist University, Dallas, Texas 75275, USA
[81]Rice University, Houston, Texas 77005, USA
[82]University of Virginia, Charlottesville, Virginia 22901, USA
[83]University of Washington, Seattle, Washington 98195, USA

We present a search for associated Higgs boson production in the process $p\bar{p} \rightarrow WH \rightarrow WWW^* \rightarrow l^{\pm}\nu l'^{\pm}\nu' + X$ in final states containing two like-sign isolated electrons or muons ($e^{\pm}e^{\pm}$, $e^{\pm}\mu^{\pm}$, or $\mu^{\pm}\mu^{\pm}$). The search is based on D0 run II data samples corresponding to integrated luminosities of 360–380 pb^{-1}. No excess is observed over the predicted standard model background. We set 95% C.L. upper limits on $\sigma(p\bar{p} \rightarrow WH) \times \mathrm{Br}(H \rightarrow WW^*)$ between 3.2 and 2.8 pb for Higgs boson masses from 115 to 175 GeV.

The Higgs boson H is a hypothesized particle introduced in the standard model (SM) that provides the mechanism by which particles acquire mass. While Higgs boson searches in the low mass region focus on the $H \rightarrow b\bar{b}$ decay mode, the $H \rightarrow WW^*$ decay mode dominates for SM Higgs boson masses above 135 GeV [1]. Furthermore, in some models with anomalous couplings ("fermiophobic Higgs boson"), the branching fraction $\mathrm{Br}(H \rightarrow W^{(*)}W^*)$ may be close to 100% for Higgs masses as low as ≈ 100 GeV [2].

In this Letter, we present a search for associated Higgs boson production ($p\bar{p} \rightarrow WH$) where the Higgs boson decays into a WW^* pair, and each of the two W bosons with the same charge decay to a charged lepton (electron or muon) plus a neutrino. The final state is characterized by two like-sign, high transverse momentum (p_T), isolated charged leptons and missing transverse energy ($\not{E}_T$) due to escaping neutrinos. This decay mode is easier to detect than $H \rightarrow b\bar{b}$, since the latter suffers from a large irreducible $Wb\bar{b}$ background. The presence of two like-sign leptons from W decays makes this channel advantageous over direct Higgs production $p\bar{p} \rightarrow H \rightarrow WW^*$, where the two leptons from W decays have opposite signs, resulting in large SM backgrounds (Z/γ^*, WW, and $t\bar{t}$ production). The main physics background in our case is $WZ \rightarrow l\nu l'l'$ and, at a much lower rate, $ZZ \rightarrow lll'l'$. The irreducible physics background, nonresonant triple vector boson production (VVV, $V = W, Z$), has a cross section that is much lower than the signal one, as does $t\bar{t} + V$.

We use data collected by the D0 detector at the Fermilab Tevatron Collider between April 2002 and August 2004. That data sample corresponds to 380 pb^{-1} of integrated luminosity in the ee channel, 370 pb^{-1} in the $e\mu$ channel, and 360 pb^{-1} in the $\mu\mu$ channel, with the variations related primarily to different trigger requirements.

The D0 detector is described in detail elsewhere [3]. Its principal elements are a central-tracking system embedded in a 2 T superconducting solenoidal magnet, a liquid-argon or uranium calorimeter, and an outer muon system. The central-tracking system consists of a silicon microstrip tracker (SMT) and a central fiber tracker (CFT) that provide tracking and vertexing for pseudorapidities $|\eta| < 3$ and $|\eta| < 2.5$, respectively [4]. The calorimeter has a central section (CC) covering $|\eta| < 1.1$ and two end calorimeters that extend coverage to $|\eta| \approx 4.2$. The outer muon system, at $|\eta| < 2$, consists of a layer of tracking

detectors and scintillation trigger counters in front of 1.8 T iron toroids, followed by two similar layers after the toroids.

The signal candidate events are selected by dilepton triggers. Off-line, the electrons are reconstructed as clusters in the electromagnetic part of the CC with central tracks pointing to them. The electron energy is measured in the calorimeter, and the tracks provide measurement of the direction and charge. The selected electromagnetic cluster candidates must be isolated in the calorimeter, have a longitudinal and transverse shower shape consistent with that of an electron, and pass a likelihood requirement that includes a spatial and momentum match between the cluster and the track, the electron track isolation, and other quantities. The muons are reconstructed in the outer muon system and matched to central tracks, their momenta being measured in the central-tracking system. They are required to be isolated, which means the minimum distance to the nearest jet in the event $\Delta R(\mu, j)$ [5] is greater than 0.5, and the scalar sum of the transverse momenta of tracks in the $\Delta R < 0.5$ cone around the muon track (excluding this track) is less than 4 GeV. Both electrons and muons are required to have transverse momenta greater than 15 GeV.

The efficiency for $WH \rightarrow WWW^* \rightarrow l^{\pm}\nu l'^{\pm}\nu' + X$ signal events to pass the selection was calculated using the PYTHIA 6.2 [6] event generator followed by a detailed simulation of the D0 detector based on the GEANT [7] package. We use the simulation to obtain the total acceptance and apply trigger and reconstruction efficiencies derived from the data. The same approach was used to simulate backgrounds from $WZ \rightarrow l\nu l'l'$ and $ZZ \rightarrow lll'l'$. These backgrounds are normalized to their next-to-leading-order cross sections calculated by the MCFM [8] program using the CTEQ6.1M parton distribution functions [9].

In addition to the physics backgrounds mentioned above, there are two types of instrumental background. One type, referred to as "charge flips," originates from the misreconstruction of the charge of one of the leptons. For the same lepton flavor channels (ee and $\mu\mu$), this background is dominated by $Z/\gamma^* \rightarrow ll$. The second type of background is like-sign lepton pairs from multijet or $W + $ jets production. In the case of muons, these can be real muons from semileptonic heavy flavor decays that pass the isolation cuts, punch-through hadrons misidentified as muons, or muons from π/K decays in flight. In the

case of electrons, the background originates from electrons in semileptonic heavy flavor decays and from γ conversions or from hadrons misidentified as electrons. This second type of background will be referred to as "QCD." There are other processes which are included in these two background categories. In particular, charge flips include events due to $WW \to l\nu l'\nu'$ production where one lepton charge is mismeasured. The decay $t\bar{t} \to ll' + X$ may contribute to either charge flips (if one of the lepton charges is mismeasured) or QCD (if a lepton from a semileptonic b decay passes the lepton identification cuts). The decay $t\bar{t} \to l + \text{jets}$ with a lepton from b decay may contribute to QCD background.

In order to reduce instrumental backgrounds, tighter track selection is needed. The lepton tracks are required to have at least 2 (out of an average of 8) SMT measurements and at least 5 (out of 16 possible) CFT measurements. Also, they must originate from the primary vertex, which is achieved by requiring the distance between the track origin and primary vertex along the beam to be less than 1 cm, the distance of closest approach (DCA) to the primary vertex in the transverse plane to be less than 0.1 cm, and the DCA significance (DCA divided by its uncertainty) to be less than 3. These cuts suppress both charge flip (due to improved track quality) and QCD (which is enriched with secondary leptons from b decays) backgrounds.

After all of these selections, we are left with a sample of 15 ee, 7 $e\mu$, and 12 $\mu\mu$ events, still dominated by instrumental background. In order to further improve the signal-to-background ratio, we perform a final selection based on a topological likelihood discriminant TLD $= \prod_i s_i / (\prod_i s_i + \prod_i b_i)$, where $s_i = s_i(\nu_i)$ and $b_i = b_i(\nu_i)$ denote probability densities of topological variables ν_i for the signal and background, respectively. The variables we use are the opening angle between the two leptons in the transverse plane $\Delta\varphi_{\mu\mu}$ ($\mu\mu$ channel), $\not{E}_T$ (ee, $e\mu$ channels), hadronic missing transverse energy ($\not{E}_T$ not corrected for lepton momenta) $\not{E}'_T$ (all channels), and the minimum angle between a lepton and $\not{E}'_T$ direction $\Delta\varphi_{l\not{E}'_T}^{\min}$ (all channels).

We consider four Higgs mass points: 115, 135, 155, and 175 GeV. For each mass, we construct an individual TLD based on variable distributions for the mass point. We optimize the TLD cut with respect to the lowest $WH \to WWW^*$ production cross section limit calculated from the expected number of events given background-only hypothesis. The contributions from SM background sources (WZ and ZZ) are computed based on their theoretical production cross sections. The shapes of the variable distributions for instrumental backgrounds are determined from data. For charge flips, we use events that pass the same selection as the signal sample, except that leptons are now required to be of unlike sign. These events are weighted according to the charge flip probability as a

function of the lepton p_T. In addition, for muons the charge mismeasurement implies that the measured p_T is not related to the original muon p_T, so the resulting distributions are convoluted with the simulated p_T distribution of mismeasured muons. For QCD, we reverse the likelihood cut for electrons and isolation cuts for muons.

The level of charge flips and QCD background contributions is determined from the fit of the dilepton invariant mass distribution to a weighted sum of the distributions for all backgrounds. To avoid potential bias from the signal, the fit is performed on a sample of events that fail the TLD cut ("complementary sample"). This procedure is performed for the ee and $\mu\mu$ channels, as illustrated in Fig. 1. We verified that the background composition is not sensitive to the actual value of the TLD cut. For the $e\mu$ channel, the background due to charge flips is *a priori* small, because $Z/\gamma^* \to ll$ production does not contribute to $e\mu$ except via $Z/\gamma^* \to \tau\tau \to e\mu +$ neutrinos. The fraction of charge flips in the $e\mu$ channel is determined from the charge flip probabilities measured in the ee and $\mu\mu$ channels. The number of background events determined on the complementary sample is converted to the background expectation in the signal sample using calculated TLD cut efficiency.

For all considered Higgs mass points, the number of events remaining after the TLD cut as a function of the cut value is consistent with expectations from the SM background, as illustrated in Fig. 2 for $M_H = 155$ GeV. For the optimal TLD cut values, 1 event in the ee channel, 3 events in the $e\mu$ channel, and 2 events in the $\mu\mu$ channel have been observed for each Higgs mass point of 135, 155, and 175 GeV. For a Higgs mass of 115 GeV, the observed
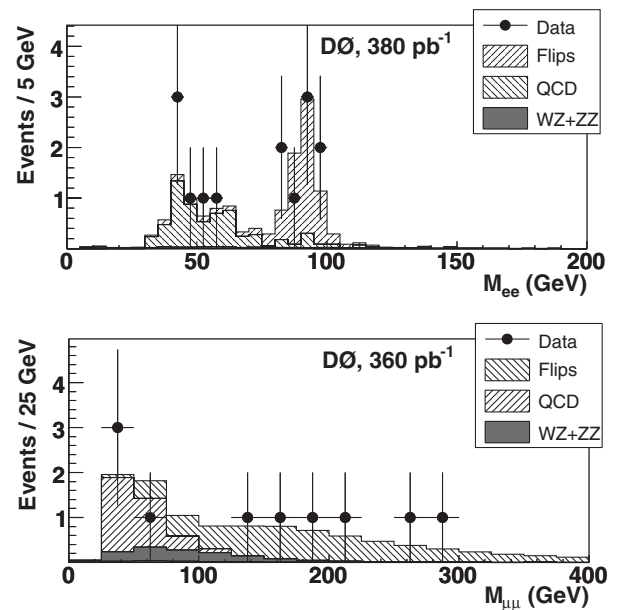

FIG. 1. The dilepton invariant mass distribution in the ee (top) and $\mu\mu$ (bottom) channels fitted to a weighted sum of the distributions for all backgrounds (for $M_H = 155$ GeV).
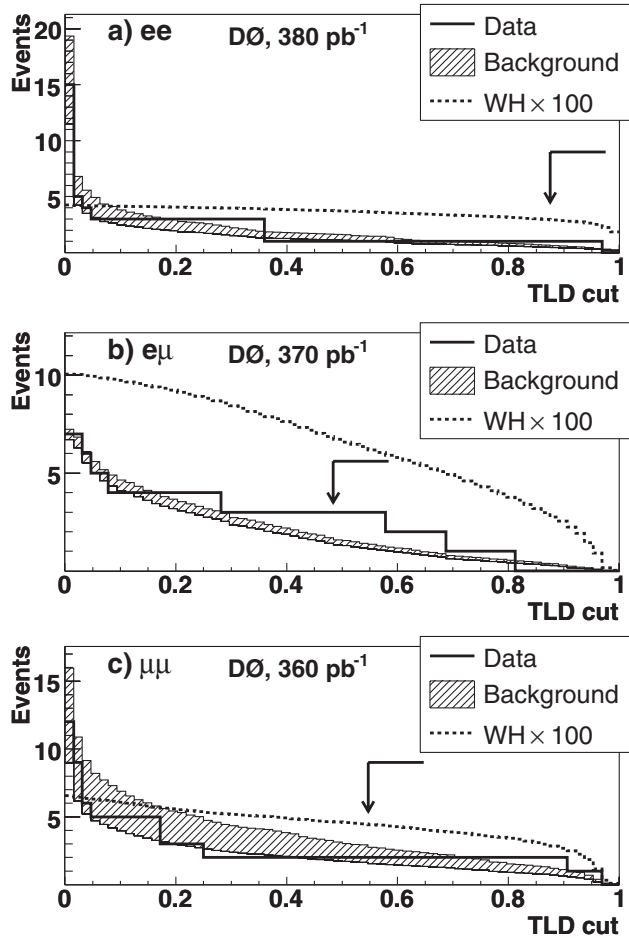
FIG. 2.   The observed number of events (solid lines), the predicted background (shaded bands), and the expected number of signal events times 100 (dashed lines) for $M_H = 155$ GeV above the TLD cut in the (a) ee, (b) $e\mu$, and (c) $\mu\mu$ channels. The width of the shaded bands corresponds to a $\pm 1\sigma$ uncertainty on the background predictions. The vertical arrows indicate the optimal cut values.

numbers of events are 1, 4, and 4, respectively, for the three channels. The number of events after the TLD cut together with the prediction for the SM background is shown in Table I.

TABLE II.   Expected and observed upper limits at the 95% C.L. for the associated Higgs boson production cross section times branching fraction $\sigma(WH) \times \mathrm{Br}(H \to WW^*)$ for various values of M_H.

M_H (GeV)	115	135	155	175
Expected limits (pb)	3.3	2.8	2.3	2.0
Observed limits (pb)	3.2	2.9	2.9	2.8

Limits on the $WH \to WWW^*$ production cross section are calculated using a ''modified frequentist'' approach described in Ref. [10]. The 95% C.L. limit is defined as the cross section at which the ratio of the confidence level for the sum of signal and background hypothesis CL_{S+B} to the confidence level for the background to represent the data CL_B reaches 0.05. The numbers of observed and expected events in the three channels are input separately to improve the sensitivity. The uncertainties on the expected numbers of signal and background events are determined from the statistical and systematic uncertainties and the luminosity uncertainty of 6.5% [11]. The signal uncertainty is 10%–11%, depending on the Higgs mass point. The main sources of the signal uncertainty are the lepton identification, 8%, and the trigger efficiency, (4–5)%. The background uncertainty is 16%–18%, dominated by the uncertainty on the composition of the instrumental background, which in turn is mostly due to the limited statistics of the complementary sample.

The expected and observed upper limits for the combination of all three channels are given in Table II. Figure 3 shows the observed upper limits together with theoretical predictions for a SM and a fermiophobic Higgs boson. No region can be excluded with the present data set.

In conclusion, a search has been performed for the process $WH \to WWW^* \to l^\pm \nu l'^\pm \nu' + X$ in the ee, $e\mu$, and $\mu\mu$ channels. In all cases, the number of observed events is in agreement with the predicted SM background. The upper limits set on $\sigma(WH) \times \mathrm{Br}(H \to WW^*)$ for the combination of all three channels vary from 3.2 to 2.8 pb as the Higgs mass varies from 115 to 175 GeV. In the case of the fermiophobic Higgs boson with a mass of 115 GeV, this

TABLE I.   Number of expected and observed events for a combination of all three channels after all selections are applied. The errors include both statistical and systematic uncertainties.

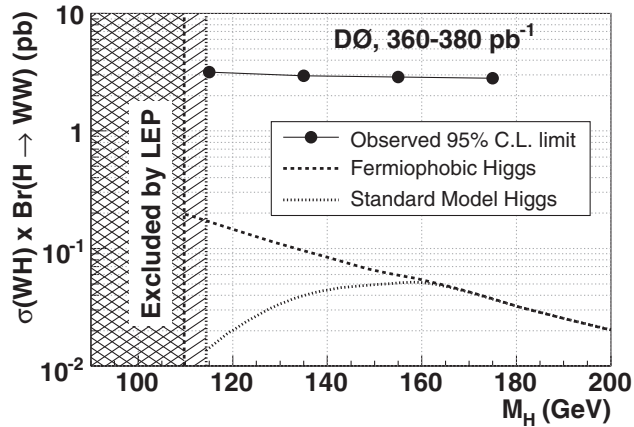| M_H (GeV)	115	135	155	175
Charge flips	2.35 ± 0.90	1.40 ± 0.53	1.12 ± 0.43	0.89 ± 0.31
QCD	2.35 ± 1.04	2.04 ± 0.83	1.64 ± 0.69	1.16 ± 0.46
WZ	3.40 ± 0.28	1.87 ± 0.15	1.51 ± 0.12	1.26 ± 0.10
ZZ	0.34 ± 0.03	0.21 ± 0.02	0.17 ± 0.01	0.15 ± 0.01
Total	8.44 ± 1.37	5.52 ± 0.99	4.45 ± 0.82	3.46 ± 0.57
Signal	0.037 ± 0.004	0.100 ± 0.010	0.143 ± 0.015	0.110 ± 0.011
Data	9	6	6	6

FIG. 3.   The observed upper limits for the four mass points along with the theoretical predictions for the SM and fermiophobic Higgs boson production. Shaded areas correspond to the LEP limits for the SM (114.4 GeV) [13] and fermiophobic (109.7 GeV) [14] Higgs boson.

represents a factor of 2.4 improvement with respect to the previous D0 result obtained in run I in the $H \rightarrow \gamma\gamma$ decay mode [12]. That becomes a factor of 22 improvement for a Higgs mass of 155 GeV.

—————

*On leave from IEP SAS Kosice, Slovakia.
†Visiting scientist from Helsinki Institute of Physics, Helsinki, Finland.
‡Visiting scientist from Lewis University, Romeoville, IL, USA.

[1] M. Spira, hep-ph/9810289.
[2] L. Brücher and R. Santos, Eur. Phys. J. C **12**, 87 (2000).
[3] V. M. Abazov *et al.*, Nucl. Instrum. Methods Phys. Res., Sect. A **565**, 463 (2006).
[4] The pseudorapidity $\eta = -\ln[\tan(\vartheta/2)]$, where ϑ is the polar angle. The D0 coordinate system has the *z* axis along the Tevatron proton beam direction.
[5] The distance ΔR is defined as $\Delta R = \sqrt{(\Delta\varphi)^2 + (\Delta\eta)^2}$, where φ is the azimuthal angle.
[6] T. Sjöstrand *et al.*, Comput. Phys. Commun. **135**, 238 (2001).
[7] R. Brun and F. Carminati, CERN Program Library Long Writeup No. W5013, 1993 (unpublished).
[8] J. M. Campbell and R. K. Ellis, Phys. Rev. D **60**, 113006 (1999).
[9] J. Pumplin *et al.*, J. High Energy Phys. 07 (2002) 012; D. Stump *et al.*, J. High Energy Phys. 10 (2003) 046.
[10] T. Junk, Nucl. Instrum. Methods Phys. Res., Sect. A **434**, 435 (1999); A. L. Read, Workshop on Confidence Limits Report No. CERN-OPEN-2000-205, 2000.
[11] T. Edwards *et al.*, Fermilab Report No. FERMILAB-TM-2278-E, 2004.
[12] B. Abbott *et al.*, Phys. Rev. Lett. **82**, 2244 (1999).
[13] R. Barate *et al.* (The LEP Working Group for Higgs Boson Searches), Phys. Lett. B **565**, 61 (2003).
[14] The LEP Working Group for Higgs Boson Searches, LHWG Note/2002-02, 2002.